AD_____

Award Number: DAMD17-01-1-0392

TITLE: The Role of the Insulin-Like Growth Factor (IGF) Binding Proteins (IGFBPs) in IGF-Mediated Tumorigenicity

PRINCIPAL INVESTIGATOR: Caroline Evangelista Harbeson
Steven A. Rosenzweig, Ph.D.

CONTRACTING ORGANIZATION: Medical University of South Carolina
Charleston, South Carolina 29425

REPORT DATE: July 2002

TYPE OF REPORT: Annual Summary

PREPARED FOR: U.S. Army Medical Research and Materiel Command
Fort Detrick, Maryland 21702-5012

REPORT DOCUMENTATION PAGE

Form Approved
OMB No. 074-0188

1. AGENCY USE ONLY (Leave blank)	2. REPORT DATE	3. REPORT TYPE AND DATES COVERED
	July 2002	Annual Summary (1 Jul 01 - 30 Jun 02)

4. TITLE AND SUBTITLE
The Role of the Insulin-like Growth Factor (IGF) Binding Proteins (IGFBPs) in IGF-mediated Tumorigenicity

5. FUNDING NUMBERS
DAMD17-01-1-0392

6. AUTHOR(S)
Caroline Evangelista Harbeson
Steven A. Rosenzweig, Ph.D. D.

7. PERFORMING ORGANIZATION NAME(S) AND ADDRESS(ES)
Medical University of South Carolina
Charleston, South Carolina 29425

E-Mail: evangelc@musc.edu

8. PERFORMING ORGANIZATION REPORT NUMBER

9. SPONSORING / MONITORING AGENCY NAME(S) AND ADDRESS(ES)
U.S. Army Medical Research and Materiel Command
Fort Detrick, Maryland 21702-5012

10. SPONSORING / MONITORING AGENCY REPORT NUMBER

11. SUPPLEMENTARY NOTES

12a. DISTRIBUTION / AVAILABILITY STATEMENT
Approved for Public Release; Distribution Unlimited

12b. DISTRIBUTION CODE

13. ABSTRACT ***(Maximum 200 Words)***

The insulin-like growth factor (IGF) system has been shown to play an important role in the progression of a number of cancers, including breast cancer. IGF-1 binds with high affinity to a family of proteins known as the IGF binding proteins (IGFBPs), which act as natural inhibitors of IGF-1 through sequestration from the IGF-1 receptor. The purpose of this proposal is the development of IGF antagonists based on the structure of the IGFBPs. Knowledge of the mechanism of IGFBP action is currently unclear, therefore we have taken a photoaffinity labeling approach to identify the IGF binding domains on the IGFBPs. Previous data collected in the lab indicate that the carboxy terminus of IGFBP-2 is involved in high affinity binding to IGF-1; these experiments are being repeated with IGFBP-3 and IGFBP-5 to extend these findings. Current photoaffinity labeling data indicate that the midregion of the IGFBP-3 protein is involved in IGF-1 binding. This information will be used in the rational design of therapeutic IGF antagonists for use in the treatment of breast and other cancers.

14. SUBJECT TERMS
cell signaling, insulin-like growth factor (IGF) binding proteins, antagonists, photoaffinity labeling

15. NUMBER OF PAGES
18

16. PRICE CODE

17. SECURITY CLASSIFICATION OF REPORT	18. SECURITY CLASSIFICATION OF THIS PAGE	19. SECURITY CLASSIFICATION OF ABSTRACT	20. LIMITATION OF ABSTRACT
Unclassified	Unclassified	Unclassified	Unlimited

Table of Contents

Annual Summary - DAMD17-01-1-0392
Caroline Evangelista Harbeson

Introduction

The insulin-like growth factor (IGF) system has been shown to play a role in the progression of breast cancer via activation of the IGF-1 receptor. IGF-1 also binds with high affinity to a family of proteins called the IGF binding proteins (IGFBPs), which serve as natural IGF-1 inhibitors through sequestration of IGF-1 from its receptor. Currently no therapeutic IGF antagonists exist. The purpose of this project is the development of novel therapeutic IGF antagonists based on the structure of the IGFBPs. A photoaffinity labeling approach is being used to identify the IGF binding domains on the IGFBPs. This information will be used in the rational design of therapeutic IGF-1 antagonists for use in the treatment of breast cancer.

Body

Specific Aim 1 as outlined in the Statement of Work involves expression of IGFBP-3 and IGFBP-5 in bacterial and mammalian expression systems. The cDNA for IGFBP-5 has been successfully cloned into an inducible bacterial expression system. The protein is produced by the bacteria, which are then lysed to collect the cell contents that contain the IGFBP. The bacteria makes the IGFBP in an unfolded state that must be treated with reducing agents (such as urea) and then carefully refolded to obtain the native, disulfide-bond containing conformation of the protein. The current yield from an average preparation from bacteria (500 ml culture) is low, however, in microgram quantities instead of the expected milligram amounts even in the presence of the inducing agent isopropyl β-D-1-thiogalactopyranoside (IPTG). The purification procedure is currently being optimized to include clones of bacteria that have demonstrated higher expression of the binding protein. The cDNA for IGFBP-3 has been successfully transfected into Chinese hamster ovary (CHO) cells for mammalian expression, which secrete the protein in its native folded and glycosylated form. Clones that express IGFBP-3 are currently being isolated and analyzed to determine protein yield. Several clones were previously isolated that expressed IGFBP-3 but these cells were lost due to contamination problems in the tissue culture facility. New clones are currently being analyzed and will be used to collect significant amounts of IGFBP-3. This expression system involves using methotrexate to induce amplification of the IGFBP-3 DNA incorporated into the mammalian chromosome. Increasing concentrations of methotrexate in the feeding media are being used to amplify the amount of protein being produced by the CHO cells. This has been a slow process because it takes time for the cells to adapt to the presence of methotrexate in their media, which initially kills a large percentage of the cells. A bacterial expression system has not been developed for IGFBP-3 as yet, and IGFBP-5 cDNA has not yet been transfected into CHO cells for mammalian expression. In the meantime, we have been purchasing recombinant IGFBP-3 in order to perform our photoaffinity labeling experiments. This form of IGFBP-3 has been prepared in bacteria and is therefore non-glycosylated. Bacterially expressed IGFBP-5 is not currently commercially available; therefore the experiments outlined using IGFBP-5 have not been performed.

Photoaffinity labeling experiments have been carried out using IGF-1 derivatized at the Gly-1 residue using 4-azidobenzoyl-N-hydroxysuccinimide ester (HSAB). This photoprobe, referred to as abGly1-IGF1, has been crosslinked to IGFBP-3 as outlined in Specific Aim 1. Mass spectrometric

analysis of the reduced and alkylated and trypsin digested photolabeled complex reveal photoincorporation of the IGF photoprobe into the midregion of the IGFBP-3 protein. This result is unexpected based on our hypothesis, which predicted that the carboxy terminus of IGFBP-3 would be identified as involved in IGF binding. The experiments with IGFBP-3 had been performed using IGF-1 derivatized using the crosslinking reagent sulfosuccinimidyl-2-[-6-(biotinamido)-2-(*p*-azidobenzamido)-hexanoamido]ethyl-1,3'-dithiopropionate (SulfoSBED), however these experiments have so far failed to yield significant mass spectrometric data. This could be due to an issue with the mass spectrometry equipment since polyacrylamide gel electrophoresis (SDS-PAGE) data indicated a significant amount of crosslinking efficiency using this IGF photoprobe (bedGly1-IGF1). These experiments are being repeated to confirm these findings, including carrying out the mass spectrometric analysis.

Specific Aim 2 of the Statement of Work involved identifying a potential site of interaction between the IGFBPs and the IGF-1 receptor binding domain on IGF-1 using crosslinking reagents attached to the Lys-27 residue of IGF-1, a residue that is located near the IGF-1 receptor binding domain. This photoprobe is known as abLys27-IGF1. Preliminary photoaffinity labeling experiments show that this photoprobe does crosslink to IGFBP-3 as seen by SDS-PAGE analysis, however the site of contact has not yet been identified by mass spectrometry. These experiments will be repeated as well, in order to identify the site of abLys27-IGF1 crosslinking to IGFBP-3. These studies will help determine if the IGFBPs interact with the receptor-binding domain on IGF-1, thus suggesting a mechanism by which the IGFBPs inhibit IGF-1 access to its receptor.

Key Research Accomplishments

- IGFBP-5 has been expressed in an inducible bacterial expression system (*E. coli*) and the purification procedure is currently being optimized.
- IGFBP-3 has been expressed in a mammalian expression system (CHO cells) and the system is currently being optimized.
- Photoaffinity labeling of IGFBP-3 using abGly1-IGF1 identified the midregion of IGFBP-3 as being involved in IGF binding.
- Photoaffinity labeling of IGFBP-3 using abLys27-IGF1 indicated that crosslinking occurred, however the site of contact has not yet been identified by mass spectrometric analysis.

Reportable Outcomes

1. At the time of submission of this proposal, we had been preparing a manuscript for publication in the Journal of Biological Chemistry. Since that time the manuscript has been reviewed and accepted (Ref. 1, Appendix 1). The data included in this paper was supported by NIH CA-78887 and Grant-in-aid S9868S from the American Heart Association to SA Rosenzweig and was used as preliminary data in preparation of this proposal. A copy of this journal article is included in the appendix section of this report.
2. The work described in this report has been presented at the 84th annual meeting of the Endocrine Society, of which I am a fellow/student member. The data was presented in poster format on June 20, 2002 in San Francisco, CA.
3. I have completed all required courses for our department as well as successfully passed a written qualifying test that examines all aspects of my course training to date. I am currently preparing for an oral examination in which I will present specific aims of my project and defend the rationale to the departmental faculty. Upon completion of these exams, I will be accepted as an official Ph.D candidate in the Dept. of Pharmacology at the Medical University of South Carolina.

Conclusions

In conclusion, several points of Specific Aim 1 of the proposed Statement of Work have been completed. IGFBP-3 has been expressed in a mammalian system, and IGFBP-5 has been expressed in a bacterial system, and both systems are currently being adjusted to promote optimal protein yield. Current photoaffinity labeling experiments with IGFBP-3 have identified the midregion of the protein as being involved in IGF-1 binding. This is an important finding because a number of studies in the literature have implicated either the carboxy or amino terminus as containing the binding site for IGF-1. While this data does not negate the importance of either of these regions of the binding proteins, it suggests that the midregion of the IGFBPs may also play an important role in IGF-1 binding. This finding is different from what we found with IGFBP-2 (Ref. 1, Appendix 1), so we can conclude that the interactions of the IGFBPs are unique to each protein in the sense that each binding protein interacts with IGF-1 using a different mechanism. In addition, the first point of Specific Aim 2 has begun, however the data has not been completely analyzed as of yet. The information gained from these studies will aid in the development of novel IGF antagonists based on the structure and function of the IGFBPs.

References

1. Horney, MJ, Evangelista, CA, and Rosenzweig, SA. Synthesis and characterization of insulin-like growth factor-1 (IGF-1) photoprobes selective for the IGFBPs: Photoaffinity labeling of the IGF-binding domain on IGF-binding protein-2 (IGFBP-2). *J. Biol. Chem.* **276**, 2880-2889, 2001.

THE JOURNAL OF BIOLOGICAL CHEMISTRY
Vol. 276, No. 4, Issue of January 26, pp. 2880–2889, 2001
Printed in U.S.A.

Synthesis and Characterization of Insulin-like Growth Factor (IGF)-1 Photoprobes Selective for the IGF-binding Proteins (IGFBPs)

PHOTOAFFINITY LABELING OF THE IGF-BINDING DOMAIN ON IGFBP-2*

Received for publication, August 17, 2000, and in revised form, October 13, 2000
Published, JBC Papers in Press, November 3, 2000, DOI 10.1074/jbc.M007526200

Mark J. Horney, Caroline A. Evangelista, and Steven A. Rosenzweig‡

From the Department of Cell and Molecular Pharmacology and Experimental Therapeutics, Medical University of South Carolina, Charleston, South Carolina 29425

Elevated insulin-like growth factor (IGF)-1 levels are prognostic for the development of prostate and breast cancers and exacerbate the complications of diabetes. In each case, perturbation of the balance between IGF-1/2, the IGF-1 receptor, and the IGF-binding proteins (IGFBPs) leads to elevated IGF-1 sensitivity. Blockade of IGF action in these diseases would be clinically significant. Unfortunately, effective IGF antagonists are currently unavailable. The IGFBPs exhibit high affinity and specificity for the IGFs and serve as natural IGF antagonists, limiting their mitogenic/anti-apoptotic effects. As an initial step in designing IGFBP-based agents that antagonize IGF action, we have begun to analyze the structure of the IGF-binding site on IGFBP-2. To this end, two IGF-1 photoprobes, $N^{\alpha Gly1}$-(4-azidobenzoyl)-IGF-1 (abG^{1}IGF-1) and $N^{\alpha Gly1}$-([2–6-(biotinamido)-2(*p*-azidobenzamido)hexanoamido]ethyl-1,3′-dithiopropionoyl)-IGF-1 (bedG^{1}IGF-1), selective for the IGFBPs were synthesized by derivatization of the α-amino group of Gly^1, known to be part of the IGFBP-binding domain. Mass spectrometric analysis of the reduced, alkylated, and trypsin-digested abG^{1}IGF-1·recombinant human IGFBP-2 (rhIGFBP-2) complex indicated photoincorporation near the carboxyl terminus of rhIGFBP-2, between residues 266 and 287. Mass spectrometric analysis of avidin-purified tryptic peptides of the bedG^{1}IGF-1·rhIGFBP-2 complex revealed photoincorporation within residues 212–227. Taken together, these data indicate that the IGFBP-binding domain on IGF-1 contacts the distal third of IGFBP-2, providing evidence that the IGF-1-binding domain is located within the C terminus of IGFBP-2.

Insulin-like growth factor (IGF)[1]-1 and IGF-2 play central roles in a number of cellular processes, including growth, proliferation, differentiation, survival, transformation, and metastasis (1, 2). Enhanced activity of the IGFs has been implicated in diabetic complications and cancer. These effects are mediated by the IGF-1 receptor (IGF-1R), a member of the receptor tyrosine kinase family of cell-surface receptors. The IGF-2 receptor, which lacks signaling activity, plays a role in clearing IGF-2 from the cell surface (3, 4). The IGFs are regulated at the extracellular level by a family of six IGF-binding proteins (IGFBPs), designated IGFBP-1–6 (5–7). These six proteins exhibit higher affinities for the IGFs than the IGF-1R, while having negligible affinity for insulin.

Renewed interest in the function of the IGF system stems from the observations that IGF-1 and IGF-2, acting through the IGF-1R, increase the tumorigenic potential of breast and prostate cancer cells (8). Accordingly, increased serum IGF-1 levels have been shown to be prognostic for the development of prostate and breast cancers (9, 10). Alterations in IGFBP expression may also contribute to disease states. For example, IGFBP-3 is a target of the p53 tumor suppressor, and a common p53 mutation results in decreased IGFBP-3 secretion (11, 12), which is likely to cause an increased proliferative response to IGF-1. Also, reduced IGFBP-2 expression resulting from the hyperglycemia of diabetes was recently shown to enhance the sensitivity of renal mesangial cells to the growth and secretory effects of IGF-1, pushing the cells toward a glomerulosclerotic phenotype (13). Because IGF-1 can suppress apoptosis, cells lacking IGF-1 receptors, cells with compromised IGF-1R signaling pathways, or cells treated with the IGFBPs may selectively die by apoptosis (8). Taken together, these findings suggest that the IGFBPs serve a role as natural IGF antagonists.

IGF-1 and IGF-2 are homologous protein hormones of 70 and 67 amino acids in length, respectively (14). Based on studies of chemically modified and mutated IGF-1, a number of residues have been identified as being part of the IGF-1R contact site, in particular the aromatic residues at positions 23–25 (15). Cooke *et al.* (16) used NMR and restrained molecular dynamics to elicit the solution structure of IGF-1; this model clearly illustrates an IGFBP-interacting domain on the surface of IGF-1 and its lack of overlap with the receptor-docking site (see Fig. 1). Specifically, this site consists of the N-terminal tripeptide Gly-Pro-Glu (17) and residues 49–51 (18). These two regions come together to form an independent binding domain (see Fig. 1) (16). The analog des-1–3-IGF-1 binds to the IGF-1R with high affinity, but has dramatically reduced affinity for the IGFBPs, underscoring the importance of the N-terminal con-

* This work was supported in part by Grant CA-78887 from the National Institutes of Health and Grant-in-aid S9868S from the American Heart Association, South Carolina Affiliate (to S. A. R.). A portion of this work was presented at the 82nd Annual Meeting of the Endocrine Society, June 21–24, 2000, Toronto, Ontario, Canada. The costs of publication of this article were defrayed in part by the payment of page charges. This article must therefore be hereby marked "*advertisement*" in accordance with 18 U.S.C. Section 1734 solely to indicate this fact.

‡ To whom correspondence should be addressed: Dept. of Cell and Molecular Pharmacology and Experimental Therapeutics, Medical University of South Carolina, 171 Ashley Ave., Charleston, SC 29425. Tel.: 843-792-5841; Fax: 843-792-2475; E-mail: rosenzsa@musc.edu.

[1] The abbreviations used are: IGF, insulin-like growth factor; IGF-1R, insulin-like growth factor-1 receptor; IGFBP, insulin-like growth factor-binding protein; rhIGFBP, recombinant human insulin-like growth factor-binding protein; HSAB, *N*-hydroxysuccinimidyl 4-azidobenzoate; SBED, sulfosuccinimidyl [2–6-(biotinamido)-2-(*p*-azidobenzamido)hexanoamido]ethyl-1,3′-dithiopropionate; abG^{1}IGF-1, $N^{\alpha Gly1}$(4-azidobenzoyl)-IGF-1; bedG^{1}IGF-1, $N^{\alpha Gly1}$-([2–6-(biotinamido)2-(*p*-azidobenzamido)hexanoamido]ethyl-1,3′-dithiopropionoyl)-IGF-1; HPLC, high performance liquid chromatography; MALDI-TOF-MS, matrix-assisted laser desorption/ionization time-of-flight mass spectrometry.

tact site on IGF-1 for binding protein specificity (17). In addition, mutations of Glu^3 or residues 49–51 result in a ligand with severely reduced binding activity (19). In good agreement with these findings, insulin lacks these residues common in the IGFBP-binding region and thus does not bind to the IGFBPs with high affinity.

The IGFBPs are globular proteins containing 18 spatially conserved cysteine residues participating in the formation of nine disulfide bonds. They range in size from 200 to 300 amino acids and, based on their high degree of homology, can be divided into three distinct domains, each constituting about one-third of the protein (20). The N- and C-terminal regions, designated domains 1 and 3, respectively, share the highest homology (20, 21), whereas the intervening region (domain 2) is highly variable (<30% homology) (6). Domains 1 and 3 contain 12 and 6 spatially conserved cysteine residues, respectively, except in the case of IGFBP-6, which is missing 2 cysteine residues in domain 1 (5); IGFBP-4 has 2 additional cysteine residues in domain 2. Because of the high homology of these proteins in domains 1 and 3 (~70%) (6), the IGF-binding domain has been proposed to reside within one of these regions. Support for this notion is based on studies in which N- or C-terminal IGFBP fragments were found to retain high affinity binding activity for IGF-1 and/or IGF-2 (19). IGFBP-related protein-1 and -2, also known as IGFBP-7/Mac25 and IGFBP-8/connective tissue growth factor, respectively, have homologies within their N termini to IGFBP-1–6 (23). These proteins have lower affinities for the IGFs compared with the IGFBPs and have been reported to interact with insulin (24). The precise mechanism by which the IGFBPs inhibit IGF-1 and IGF-2 action is presently unknown. It is thought to involve high affinity binding of the IGFs by the IGFBPs, thereby limiting their access to the IGF-1R. A complete understanding of this inhibitory action will come with the solution of the three-dimensional structure of the IGFBPs. As of yet, the IGF-binding domain on the IGFBPs has not been defined.

To date, extensive use of molecular techniques has been applied to assess the binding domain on the IGFBPs. However, only sparse structural information has been obtained. Currently, a debate exists as to which domain(s) of the IGFBPs are most crucial for IGF binding. This is further confounded by the paucity of precise structural information about the IGFBPs as recently reviewed by Baxter (25). To more precisely identify the points of contact between IGF-1 and IGFBP-2, we chose to pursue a photoaffinity labeling approach, which has been used to identify sites of interaction between a number of interacting proteins. On this basis, we derivatized the α-amino group of the N-terminal glycine of IGF-1 with two different photoaffinity reagents, *N*-hydroxysuccinimidyl 4-azidobenzoate (HSAB) and sulfosuccinimidyl [2–6-(biotinamido)-2-(*p*-azidobenzamido)-hexanoamido]ethyl-1,3′-dithiopropionate (SBED), to generate IGF-1 photoprobes capable of selectively labeling the IGF-binding domain on IGFBP-2. The advantage of this approach is that the photoreactive group is inserted within the region shown to be essential for high affinity binding of IGF-1 to the IGFBPs. Since IGF-2, which has a 3-residue N-terminal extension, exhibits a higher affinity for IGFBP-2 than IGF-1, reduced binding affinity of IGF-1 for IGFBP-2 resulting from N-terminal substitutions was not anticipated. In this study, we describe the synthesis and characterization of $N^{\alpha Gly1}$-(4-azidobenzoyl)-IGF-1 (abG^{1}IGF-1) and $N^{\alpha Gly1}$-([2–6-(biotinamido)-2-(*p*-azidobenzamido)hexanoamido]ethyl-1,3′-dithiopropionoyl)-IGF-1 (bedG^{1}IGF-1) and their successful application to photoaffinity label rhIGFBP-2. Based on these direct photoaffinity labeling analyses, our results indicate that the C terminus of IGFBP-2 contains the IGF-binding domain.

EXPERIMENTAL PROCEDURES

Materials—Recombinant human IGF-1 was provided by Genentech, Inc. (South San Francisco, CA). HSAB was synthesized from *p*-aminobenzoic acid, sodium azide (Sigma),and dicyclohexylcarbodiimide (Pierce) and purified according to the method of Galardy *et al.* (26). HPLC columns were from Vydac Instruments (Hesperia, CA). SBED, UltraLink™ monomeric avidin-agarose, NeutrAvidin™-peroxidase, and tris(2-carboxyethylyl)phosphine hydrochloride were obtained from Pierce. Methotrexate was from Immunex Corp. (Seattle, WA), and fetal bovine serum was from Summit Biotechnology (Fort Collins, CO). cDNA encoding human IGFBP-2 (27) was obtained from Dr. Jörg Landwehr (Hoffmann-La Roche, Basel, Switzerland). All other materials were of reagent grade or higher.

Synthesis and Purification of abG^{1}IGF-1 and bedG^{1}IGF-1—All derivatizations and handling of photoprobes were carried out under subdued lighting or under a red safety light. abG^{1}IGF-1 was synthesized by reaction of recombinant human IGF-1 (1 mg, 130 nmol) with a 10-fold molar excess of HSAB (0.34 mg, 1.3 μmol) for 1 h at 23 °C. Unreacted ester was quenched by the addition of 30 μl of ethanolamine for 30 min, and the entire reaction mixture was lyophilized. The lyophilized reaction mixture was dissolved in 0.5 M acetic acid and 10 μl of trifluoroacetic acid and injected onto a C_{18} column equilibrated in 0.1% trifluoroacetic acid and 24% acetonitrile at a flow rate of 1 ml/min. After 20 min, a linear gradient of 24–60% acetonitrile was developed over 60 min to elute IGF-1 and the reaction products. Peak 4 was collected, dried *in vacuo* in a SpeedVac concentrator (Savant Instruments, Inc., Farmingdale, NY), reinjected onto the C_{18} column equilibrated in 50 mM triethanolamine phosphate (pH 3.0) containing 27.5% acetonitrile, and eluted with a gradient of 27.5–38% acetonitrile over 60 min. The major peak was collected, dried, and further analyzed. Synthesis and purification of bedG^{1}IGF-1 was carried out essentially as described for abG^{1}IGF-1 using a 1:1 ratio of SBED to protein.

Pepsin Digestion of abG^{1}IGF-1 and bedG^{1}IGF-1—IGF-1 and the photoprobes were digested with pepsin at an enzyme/substrate ratio of 1:20 in 0.01 M HCl for 5 h at 23 °C (28). Digests were then injected onto a C_{18} column equilibrated in 0.1% trifluoroacetic acid, and the fragments were eluted using a linear gradient of 0–60% acetonitrile over 90 min. For each photoprobe, the HPLC fractions containing fragments with potentially modified residues (AE, CG, and D fragments) (see Fig. 3) (28) were analyzed by matrix-assisted laser desorption/ionization time-of-flight mass spectrometry (MALDI-TOF-MS).

MALDI-TOF-MS—Dried HPLC fractions were dissolved in 0.1% trifluoroacetic acid containing 70% acetonitrile. 0.5-μl aliquots of each fraction were mixed with 1 μl of 50 mM α-cyano-4-hydroxycinnamic acid (Sigma) in 0.1% trifluoroacetic acid and 70% acetonitrile. The mixture was spotted onto a gold-coated, stainless steel sample plate and air-dried. The samples were analyzed using a PerSeptive Biosystems Voyager-DE MALDI-TOF mass spectrometer equipped with a 337-nm nitrogen laser. A delayed extraction source was operated in linear mode (1.2-m ion flight path, 20-kV accelerating voltage), yielding an instrumental resolution of ~700 (full width at half-maximum) at m/z 1297.5. One mass spectrum was based on 256 averaged mass scans. External mass calibration was performed using angiotensin I (1297.5 Da) and bovine insulin (5734.54 Da) as standards. Mass accuracy was ±0.1%.

Purification of rhIGFBP-2—rhIGFBP-2 was purified from DHFR$^-$ Chinese hamster ovary cells (29) stably transfected with 30 μg of pCMV-hIGFBP-2 and 2 μg of pMT2 containing murine dihydrofolate reductase (30) using calcium phosphate. Cells were grown to confluence in roller bottles and subjected to a weekly cycle of 3 days growth in serum-containing medium, followed by 4 days in serum-free medium. Pooled conditioned medium (400–600 ml) was acidified to pH 3–4 with glacial acetic acid and dialyzed against 10 mM acetic acid in Spectrapor 4 membranes (12,000–14,000 M_r cutoff; Spectrum, Laguna Hills, CA) to remove salt and IGFs. After lyophilization, IGFBP-2 was purified by sequential IGF-1-agarose affinity chromatography and reversed-phase HPLC on a C_4 column equilibrated in 0.1% trifluoroacetic acid. IGFBP-2 eluted between 30 and 40% acetonitrile.

IGF-1-Agarose Affinity Chromatography—2 ml of Affi-Gel 10-activated immunoaffinity support (Bio-Rad) were washed four times with 3 volumes of cold water, followed by the addition of 2 mg of IGF-1 in 100 mM HEPES (pH 7.4). The mixture was agitated overnight at 4 °C, followed by two washes with 100 mM HEPES (pH 8.0). Unreacted sites were then quenched with 2 ml of 1 M Tris-HCl (pH 7.9) for 1 h at ambient temperature. The column was then washed with three cycles of alternating low pH/high pH salt washes (0.5 M NaCl and 0.1 M sodium acetate (pH 4.0) and 0.5 M NaCl and 0.1 M Tris (pH 8.0), respectively). Finally, the column was washed and stored in 10 ml of 150 mM NaCl

and 50 mM HEPES (pH 7.4) with 0.05% sodium azide.

Dialyzed and lyophilized conditioned medium was dissolved in 40–45 ml of 50 mM HEPES (pH 7.4) containing 150 mM NaCl (Buffer A). Insoluble material was removed by centrifugation at 3000 × *g* for 20 min. 2 ml of IGF-1-agarose in Buffer A were then added, and the slurry was incubated overnight at 4 °C with gentle agitation. The column was subsequently washed with 100 ml of Buffer A, followed by 50 ml of 10% Buffer A. Proteins bound to the column were then eluted with 15 ml of 0.5 M acetic acid, and the column was washed with 20 ml of Buffer A plus 1 ml of 1 M HEPES (pH 7.4), followed by 40 ml of Buffer A. The eluate was dried *in vacuo* using a SpeedVac concentrator. The dried eluate was stored at −20 °C until further purification as described above.

IGFBP-2 Binding Assay—Soluble IGFBP-2 binding assays were carried out using polyethylene glycol precipitation and centrifugation (31). 1 ng of rhIGFBP-2 was combined with various concentrations of IGF-1, abG^{1}IGF-1, or bedG^{1}IGF-1 ranging from 30 fM to 100 nM in binding assay buffer (100 mM HEPES (pH 7.4), 44 mM $NaHCO_3$, 0.01% bovine serum albumin, 0.01% Triton X-100, and 0.02% NaN_3), followed by the addition of 10 nCi of ^{125}I-IGF-1 (Amersham Pharmacia Biotech). After a 4-h incubation at room temperature, 250 μl of 0.5% bovine γ-globulin were added, followed by 500 μl of 25% polyethylene glycol (average M_r of 8000; Sigma). The samples were incubated for 10 min at room temperature and centrifuged for 3 min at 15,000 × *g*. The pellets were washed with 1 ml of 6.25% polyethylene glycol, and bound radioactivity was quantified in a Compugamma spectrometer (LKB-Wallac, Turku, Finland). Counts bound in the presence of 1 μM or 100 nM IGF-1 (nonspecific binding) were subtracted to obtain specific binding. IC_{50} values were calculated using the equation $B = B_{max}/(1 + [\text{ligand}]/IC_{50})$, where B is the concentration of bound ligand and B_{max} is the maximal binding observed. The Microsoft Excel 97 Solver was used to minimize the sum of the squares of the differences from the mean IC_{50} values for each IGF-1 concentration by optimizing B restrained by the above equation. The calculated IC_{50} values were used to generate smooth curves.

Photoaffinity Labeling—Equimolar quantities of abG^{1}IGF-1 or bedG^{1}IGF-1 and rhIGFBP-2 were allowed to attain equilibrium binding by co-incubation for 4 h at 23 °C in 100 mM HEPES (pH 7.4) containing 44 mM $NaHCO_3$ and 0.01% Triton X-100. The sample was then placed in ice water and irradiated for 2 h with a prewarmed Fotodyne handheld, single-wavelength UV lamp (2 × 4-watt 300-nm bulbs) at a distance of 2 cm. The mixture was dried *in vacuo*, and the proteins were reduced and alkylated using tris(2-carboxyethylyl)phosphine (32) and 4-vinylpyridine (33). abG^{1}IGF-1- and bedG^{1}IGF-1-photolabeled IGFBP-2 proteins were separated from unreacted IGFBP-2 by reversed-phase HPLC and trypsinized as described below.

Trypsinization of IGF-1, IGFBP-2, and Photoaffinity-labeled Complexes—Trypsinization of reduced and alkylated proteins was performed according to Honegger and Humbel (34). Proteins (20 μM) were dissolved in 100 mM *N*-ethylmorpholine acetate (pH 8.5) to which was added sufficient trypsin (1 μg/μl) to achieve a 1:50 enzyme/substrate ratio. Mixtures were then incubated for 2 h at 37 °C, followed by a second addition of trypsin. After 2 additional h at 37 °C, the reaction was stopped by the addition of an equal volume of 0.1% trifluoroacetic acid. The mixture was dried *in vacuo* or applied directly to a C_{18} reversed-phase HPLC column.

Avidin Chromatography of bedG^{1}IGF-1·IGFBP-2 Tryptic Peptides—Tryptic peptides generated from the bedG^{1}IGF-1·IGFBP-2 complex were applied to an UltraLink™ monomeric avidin column. Flow-through fractions were collected and pooled. The column was eluted with low pH buffer, and the eluate fractions were pooled. The flow-through and eluate fractions were dried and further analyzed by reversed-phase HPLC on a C_{18} column equilibrated in 0.1% trifluoroacetic acid and eluted with a linear gradient of acetonitrile. Eluted peaks were analyzed by MALDI-TOF-MS.

Immunoblots—Samples were dissolved in SDS sample buffer with or without dithiothreitol and resolved on a 10 or 12.5% SDS-polyacrylamide gel according to the procedure of Laemmli (35) using a Hoefer Scientific Instruments apparatus. The proteins were transferred to nitrocellulose and immunoblotted using a commercial antiserum against intact bovine IGFBP-2 (Upstate Biotechnology, Inc., Lake Placid, NY). Blots were developed with horseradish peroxidase-labeled secondary antibody (Chemicon International, Inc., Temecula, CA) and an enhanced chemiluminescence kit (Amersham Pharmacia Biotech). For sequential anti-IGF-1/anti-IGFBP-2 antibody analysis of the same blot, the membrane was stripped for 20 min at 60 °C in 1 M Tris (pH 6.7) containing 10% SDS and 0.1 M β-mercaptoethanol. The stripped membrane was washed twice with Tris-buffered saline containing Tween for 10 min at 23 °C, followed by blocking for 1 h with 5% nonfat dry milk and reprobed.

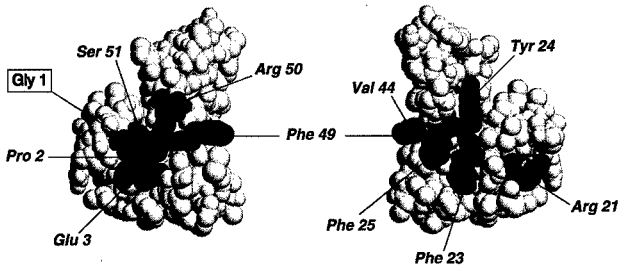

FIG. 1. **IGFBP-binding site on IGF-1.** *Left*, the N-terminal residues Gly^1, Pro^2, and Glu^3 combine with Phe^{49}, Arg^{50}, and Ser^{51} to form the IGFBP-binding domain (6). Note that the Gly^1 α-NH_2 group is the site chosen for derivatization with aryl azide-based photoaffinity reagents. *Right*, the IGF-1R-binding domain on IGF-1. The image was obtained by RasMol Version 2.6 using coordinates (6) from the Protein Data Bank, Research Collaboratory for Structural Bioinformatics, Rutgers University (New Brunswick, NJ).

RESULTS

Synthesis and Purification of abG^{1}IGF-1 and bedG^{1}IGF-1—As shown in Fig. 1, the three-dimensional structure of IGF-1 reveals the presence of distinct binding domains for the IGFBPs and the IGF-1R, which do not overlap. IGF-1 contains four primary amines (the ε-amino groups of 3 lysyl residues and the α-amino group of Gly^1), all of which are reactive with HSAB and SBED. Fig. 2 shows the structures of these reagents and highlights the relative lengths of the spacer arms from the site of covalent linkage to IGF-1 to the photoreactive azide group. In addition to a significantly longer spacer arm, SBED also contains a reduction-sensitive disulfide linkage and a biotin moiety. As a result, although we anticipated that use of HSAB as a photocross-linking agent would yield a reduction-stable covalent IGF-1·IGFBP-2 complex, use of SBED was expected to produce a reduction-sensitive IGF-1·IGFBP-2 complex that, after reduction, would result in biotinylation of IGFBP-2 at the site of photoincorporation.

As shown in Fig. 2, reaction of HSAB and SBED with IGF-1 as described under "Experimental Procedures" resulted in production of three major products (peaks 2–4) in addition to unreacted IGF-1 (peak 1). Analysis of the HSAB reaction products by acidic polyacrylamide gel electrophoresis in 8 M urea and by MALDI-TOF-MS revealed that these three peaks were monoderivatized forms of IGF-1 (data not shown). Peak 2 had previously been shown to represent the elution position of abK^{27}IGF-1 (where K^{27} is Lys^{27}) (36). Peaks 3 and 4 had been tentatively identified as abK^{65}IGF-1 and abG^{1}IGF-1, respectively, based on amino acid sequencing analysis (36). No abK^{68}IGF-1 was detected. The three product peaks were further purified by chromatography on a C_{18} column equilibrated in triethanolamine phosphate and acetonitrile. Structural assignments were confirmed using pepsin digestion as described below. After derivatization with SBED, peaks 2–4 were shown to similarly represent bedK^{27}IGF-1, bedK^{65}IGF-1, and bedG^{1}IGF-1 (Fig. 2*B*).

Characterization of abG^{1}IGF-1 and bedG^{1}IGF-1—To verify that the "ab" and "bed" moieties were covalently bound to the α-amino group of Gly^1 for each photoprobe, it was necessary to isolate Gly^1 from the 3 Lys residues. Since reduction and alkylation might disrupt the azide moiety, we utilized pepsin digestion of nonreduced abG^{1}IGF-1 and bedG^{1}IGF-1. As reported by Forsberg *et al.* (28) and shown in Fig. 3, pepsin releases a disulfide-linked AE fragment containing Gly^1 and no Lys residues. Pepsin digestion of abG^{1}IGF-1 and bedG^{1}IGF-1 was

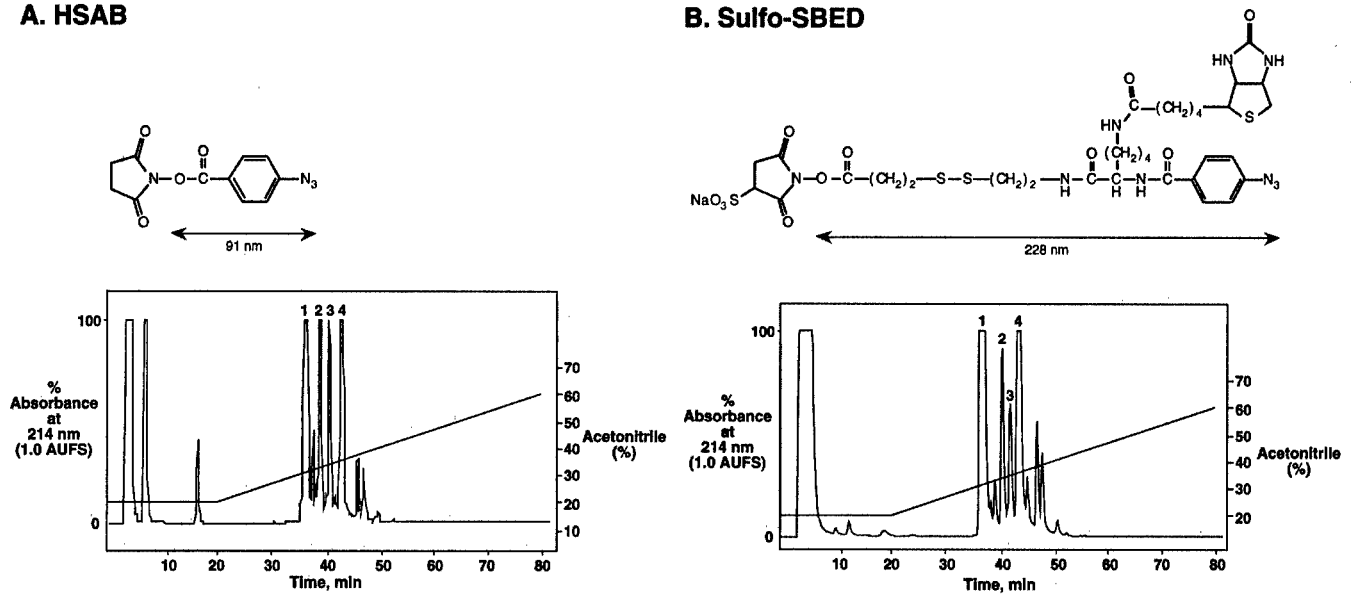

FIG. 2. **Synthesis of $N^{\alpha Gly1}$-derivatized IGF-1 photoprobes.** Shown above each chromatogram are the structures of the photoreagents used to derivatize IGF-1. Below are the elution profiles of the reaction products obtained on a C_{18} reversed-phase column. Typically, four major products were obtained in each reaction. For each probe, peak 4 was collected from each of two separate synthesis reactions pooled, ,dried and rechromatographed on a C_{18} column as described under "Experimental Procedures." *A*, derivatization with HSAB; *B*, derivatization with SBED. Each HPLC chromatogram shown is representative of four independent synthesis reactions. *AUFS*, absorbance units at full scale.

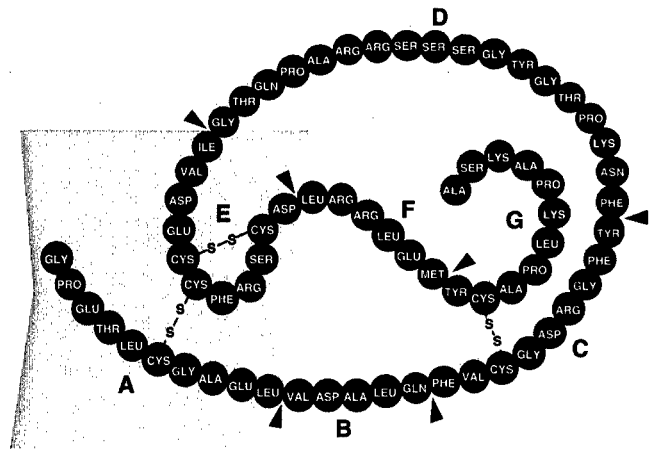

FIG. 3. **Pepsin cleavage sites in IGF-1.** To verify derivatization of IGF-1 at its N-terminal glycine residue, purified probes were digested with pepsin. The primary sequence of IGF-1 is shown, with *arrowheads* indicating the primary sites of pepsin cleavage (28). *Letters A–G* indicate the principal peptides generated. The disulfide-linked AE fragment (*shaded*) contains the N-terminal glycyl residue and none of the lysyl residues.

carried out in the dark to avoid photoactivation of the probe, and recombinant human IGF-1 was also digested in parallel to serve as a control for subsequent HPLC and mass spectrometric analyses.

For each photoprobe, HPLC purification of the pepsin digestion products revealed that the retention times for the derivatized AE fragments were significantly increased compared with the underivatized AE fragment (data not shown). This was predicted based on the added hydrophobicity of the additional functional groups. Fig. 4*A* shows the MALDI-TOF-MS of abG^1AE. This fragment had the correct mass (predicted average mass of 2419.7 Da; observed mass of 2419.8 Da) and exhibited loss of nitrogen as a result of photoactivation by the 337-nm laser, to yield a second peak at 2394.3 Da. The identities of the CG and D fragments, containing Lys^{65}/Lys^{68} and Lys^{27}, respectively, were also confirmed by MALDI-TOF-MS and were in good agreement with those of Forsberg *et al.* (28). Similar observations were made for $bedG^1IGF$-1. As shown in Fig. 5, a peak at 2956.2 Da (predicted average mass of 2955.9 Da) was observed along with a second peak at 2929.4 Da, reflecting the loss of nitrogen resulting from photolysis. Again, the CG and D fragments exhibited masses consistent with a lack of derivatization. As an alternate method of validation of the derivatization, electrospray ionization MS^3 was also carried out (data not shown).

Having demonstrated the structure and purity of abG^1IGF-1 and $bedG^1IGF$-1, it was necessary to ensure that each probe retained high affinity binding for IGFBP-2 similar to that of native IGF-1. The results of IGFBP-2 competition binding assays are shown in Fig. 6. The IC_{50} values for IGF-1, abG^1IGF-1, and $bedG^1IGF$-1 were 173, 131, and 168 pM, respectively, indicating that the photoprobes and IGF-1 had identical affinity for IGFBP-2. These data indicate that the addition of the photoreactive group does not significantly hinder the IGF-1/IGFBP-2 interaction.

Photoaffinity Labeling of IGFBP-2—Photoaffinity labeling of IGFBP-2 with abG^1IGF-1 and $bedG^1IGF$-1 was carried out as described under "Experimental Procedures." In a small-scale photolabeling study with abG^1IGF-1, an aliquot of the reaction mixture was subjected to immunoblot analysis with anti-IGFBP-2 and anti-IGF-1 antisera under reducing conditions (Fig. 7*A*). In addition to rhIGFBP-2 migrating at ~32 kDa and detected by anti-IGFBP-2 antiserum, a second protein species migrating at ~40 kDa was detected. This band reacted with both anti-IGF-1 and anti-IGFBP-2 antibodies, indicating that the photoaffinity labeling reaction had successfully generated abG^1IGF-1·IGFBP-2 complexes. These data confirm that photolabeling of IGFBP-2 with abG^1IGF-1 results in a stable covalent IGF-1·IGFBP-2 complex that is not disrupted by reduction.

A similar analysis was carried out for $bedG^1IGF$-1 (Fig. 7*B*). As shown in *lane 1*, two bands were detected with anti-IGFBP-2 antiserum: IGFBP-2 itself and the $bedG^1IGF$-1·IGFBP-2 complex. This complex bound to and was specifically eluted from an avidin-agarose column, whereas IGFBP-2 did not bind at all (*lane 2*). Under nonreducing conditions, NeutrAvidin™-peroxidase was unable to detect the $bedG^1IGF$-1·IGFBP-2 complex (*lane 3*). In *lanes 4–6*, the $bedG^1IGF$-1·IGFBP-2

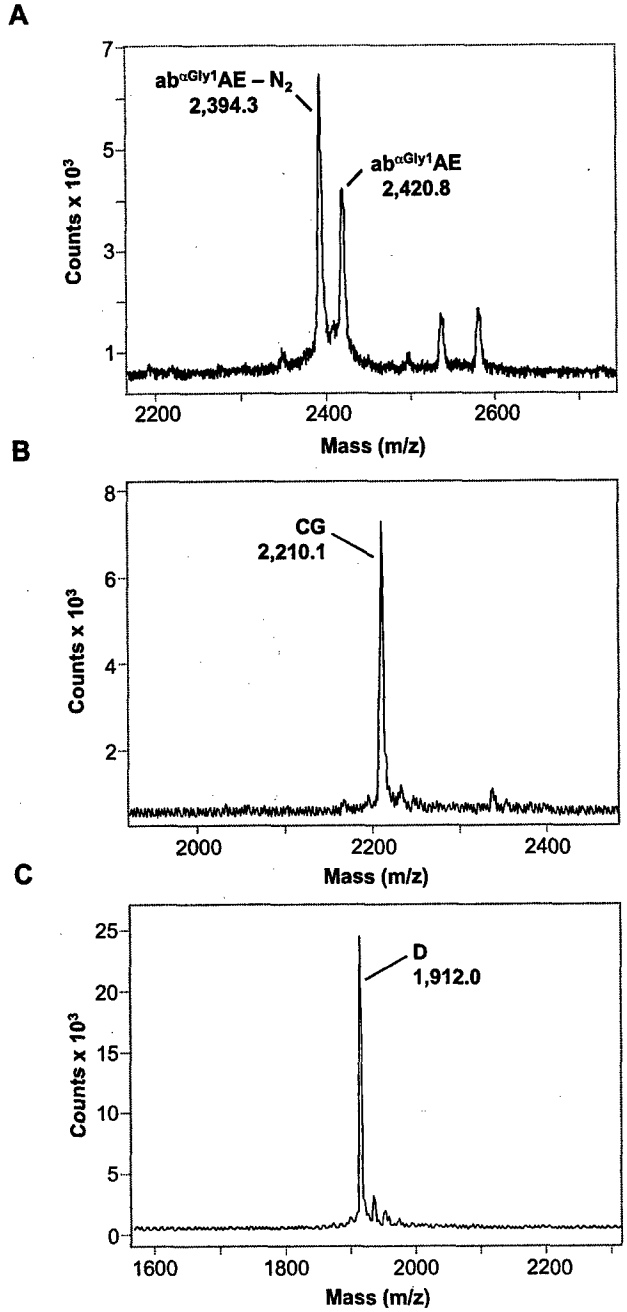

FIG. 4. **Characterization of abG^{1}IGF-1 by pepsin digestion.** The AE (*A*), CG (*B*), and D (*C*) fragments of abG^{1}IGF-1 were purified by HPLC and analyzed by MALDI-TOF-MS.

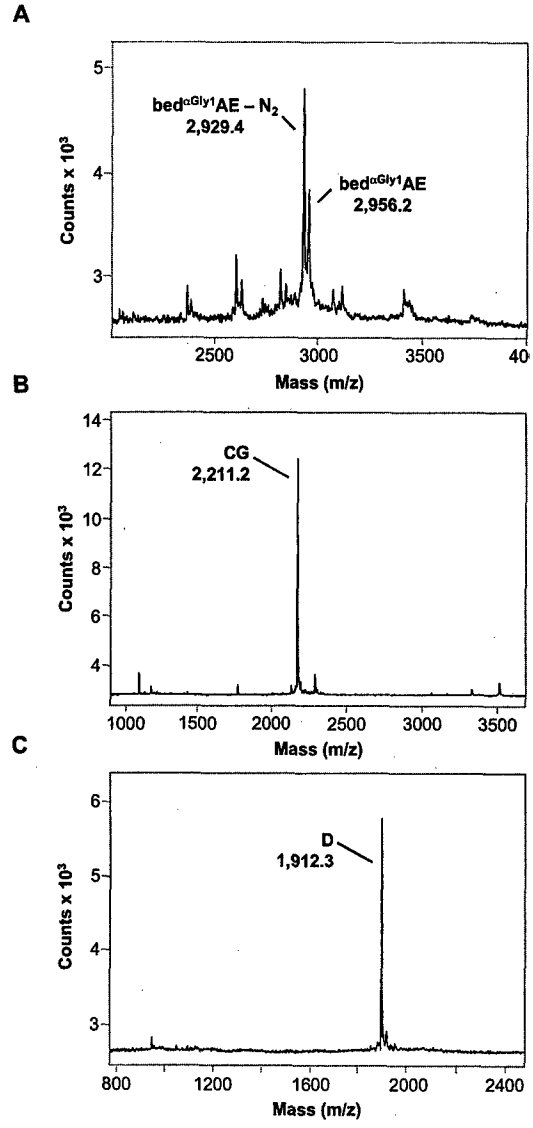

FIG. 5. **Characterization of bedG^{1}IGF-1 by pepsin digestion.** The AE (*A*), CG (*B*), and D (*C*) fragments of bedG^{1}IGF-1 were purified by HPLC and analyzed by MALDI-TOF-MS.

complex was first reduced and alkylated with tris(2-carboxyethylyl)phosphine and 4-vinylpyridine prior to electrophoresis. As discussed above, reduction and alkylation of bedG^{1}IGF-1·IGFBP-2 should yield IGFBP-2 biotinylated at the site of photoincorporation. As shown in *lanes 4–6*, two bands were again detected with reduction and alkylation of the samples. The upper band had the same electrophoretic mobility as uncross-linked, reduced, and alkylated IGFBP-2 and was detectable with anti-IGFBP-2 antibodies. However, roughly one-half of the content of this band was retained on the avidin-agarose column (*lane 5*) and reacted with NeutrAvidin™-peroxidase (*lane 6*), indicating that the band in *lane 4* contains both unreacted and biotinylated IGFBP-2. The lower band reacted with anti-IGFBP-2 antibodies, was retained by the avidin-agarose column (*lane 5*), and could be labeled with NeutrAvidin™-peroxidase (*lane 6*), indicating that it represents a biotinylated fragment of IGFBP-2. These results indicate that reduction of the bedG^{1}IGF-1·IGFBP-2 complex allowed greater access of avidin-peroxidase to the biotin moiety on photolabeled IGFBP-2.

Identification of the abG^{1}IGF-1 Photoincorporation Site—To identify the site of photoincorporation of abG^{1}IGF-1, the abG^{1}IGF-1·IGFBP-2 complex was isolated by HPLC following reduction and alkylation of the photolysis reaction mixture. Owing to the similar retention times of the free and cross-linked species, the two components overlapped significantly (Fig. 8*A*). Subsequent re-chromatography of each component provided sufficient resolution to attain a high level of purification of the abG^{1}IGF-1·IGFBP-2 complex (Fig. 8*B*). Immunoblot analysis of the column fractions indicated that >40% photoincorporation was achieved.

Fractions containing purified abG^{1}IGF-1·IGFBP-2 were pooled, dried, and trypsinized. It was anticipated that tryptic digestion of the abG^{1}IGF-1·IGFBP-2 complex would yield a cross-linked peptide containing a tryptic fragment of IGFBP-2 (BP2T) and the N-terminal tryptic fragment of abG^{1}IGF-1 (abIGF1T). Since abIGF1T alone (residues 1–21) is 2521 Da, this represents the minimum mass for the resulting cross-linked peptide (BP2T-abIGF1T). The tryptic digest was applied

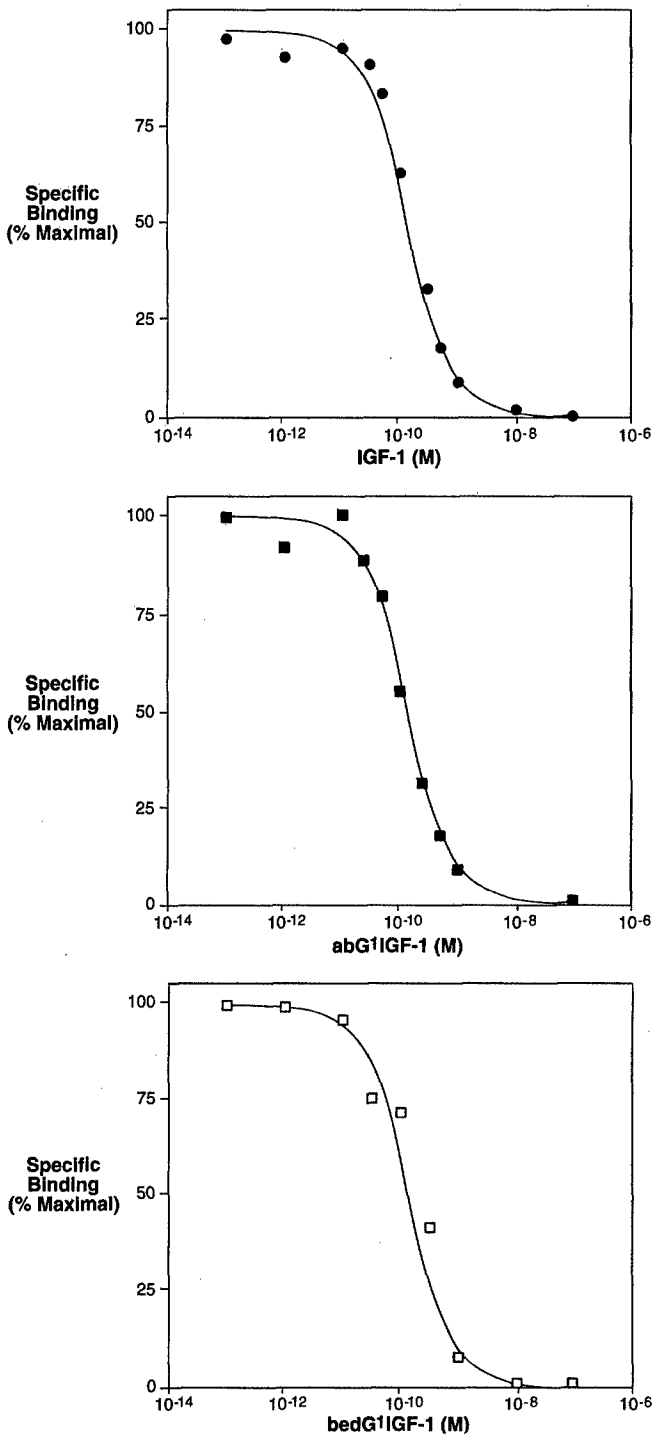

FIG. 6. **Competition binding analyses of $N^{\alpha Gly1}$-derivatized photoprobes.** The binding activities of the IGF-1 photoprobes were analyzed with a polyethylene glycol precipitation-based assay using IGF-1 (●), abG^{1}IGF-1 (■), or bedG^{1}IGF-1(□) to compete with ^{125}I-IGF-1 for binding to IGFBP-2 (see "Experimental Procedures"). Data points shown are average values of two independent experiments performed in triplicate. Binding curves were generated as described under "Experimental Procedures."

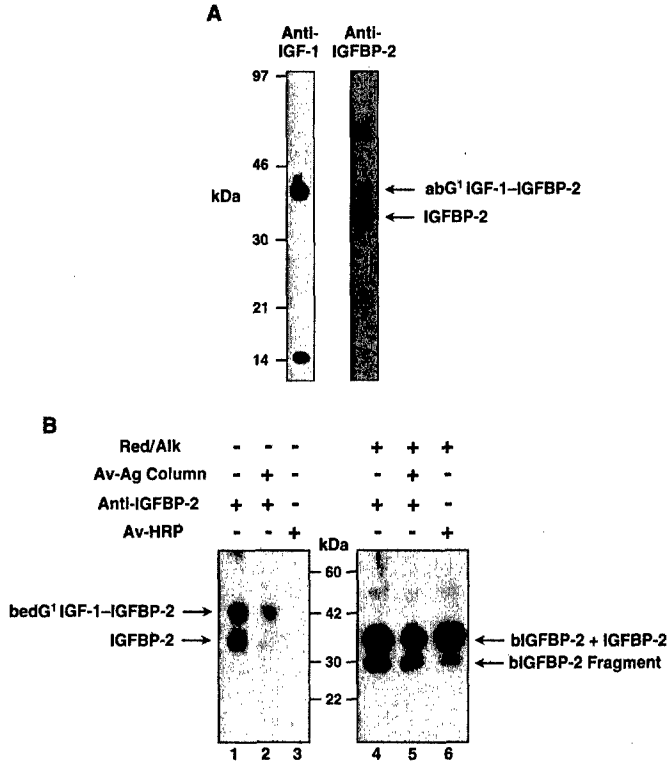

FIG. 7. **Analysis of photoaffinity-labeled complexes.** *A*, abG^{1}IGF-1-labeled complexes were resolved on an SDS gel and transferred to nitrocellulose. The blot was probed with anti-IGFBP-2 antibodies, followed by stripping and reprobing with anti-IGF-1 antibodies. *B*, products of photoaffinity labeling with bedG^{1}IGF-1 were immunoblotted with a polyclonal anti-IGFBP-2 antibody or probed with NeutrAvidin™-peroxidase (*Av-HRP*) as indicated. Some aliquots were applied to an UltraLink™ avidin-agarose (*Av-Ag*) column; the low pH eluate was run on the gel. *Red/Alk*, reduction and alkylation.

to a C_{18} column and eluted with a shallow gradient of acetonitrile to obtain optimal separation of the tryptic peptides (data not shown). MALDI-TOF-MS was then performed on each fraction to locate BP2T-abIGF1T. The MALDI mass spectrum of the identified fraction is shown in Fig. 9*A*. Although not pure, we obtained a significant enrichment of BP2T-abIGF1T in this fraction with an observed mass of 5295.6 Da. These results suggest that abIGF1T (predicted mass of 2521 Da) was covalently incorporated into the C-terminal tryptic peptide of IGFBP-2 corresponding to residues 266–287 (BP2T predicted mass of 2772 Da), yielding a complex with a predicted mass of 5293 Da. To further validate this assignment, the fraction containing this complex was subdigested with *Staphylococcus aureus* V8 protease and analyzed by MALDI-TOF-MS. As illustrated in Fig. 9 (*B* and *C*), MALDI-TOF-MS of this fraction identified four distinct peptides consistent with the proposed structure. These data indicate that when attached to the α-amino group of Gly^1, the azidobenzoyl moiety contacts IGFBP-2 in its distal C-terminal end within the tryptic peptide corresponding to residues 266–287 (see Fig. 11*A*).

Identification of the bedG^{1}IGF-1 Photoincorporation Site—To determine the site of photoincorporation of bedG^{1}IGF-1 into IGFBP-2, the photolyzed reaction mixture obtained as described under "Experimental Procedures" was reduced and alkylated with tris(2-carboxyethylyl)phosphine and 4-vinylpyridine, resulting in cleavage of IGF-1 from the complex and biotinylation of IGFBP-2 at the site of photoincorporation. The mixture was then desalted on a C_4 column, dried *in vacuo*, and digested with trypsin. The tryptic peptides were loaded onto an UltraLink™ monomeric avidin column, which was washed with 6 column volumes of phosphate-buffered saline. To release retained biotinylated tryptic peptides, the column was eluted with regeneration buffer (0.2 M glycine (pH 2.8)). The flow-through/washes and eluate fractions were pooled separately and dried, and the peptides present in each were resolved by HPLC on a C_{18} column. As expected, the majority of peptides eluted in the flow-through fraction of the avidin column (Fig. 10*A*), resembling a representative combined tryptic digest of uncross-linked IGF-1 and IGFBP-2 (data

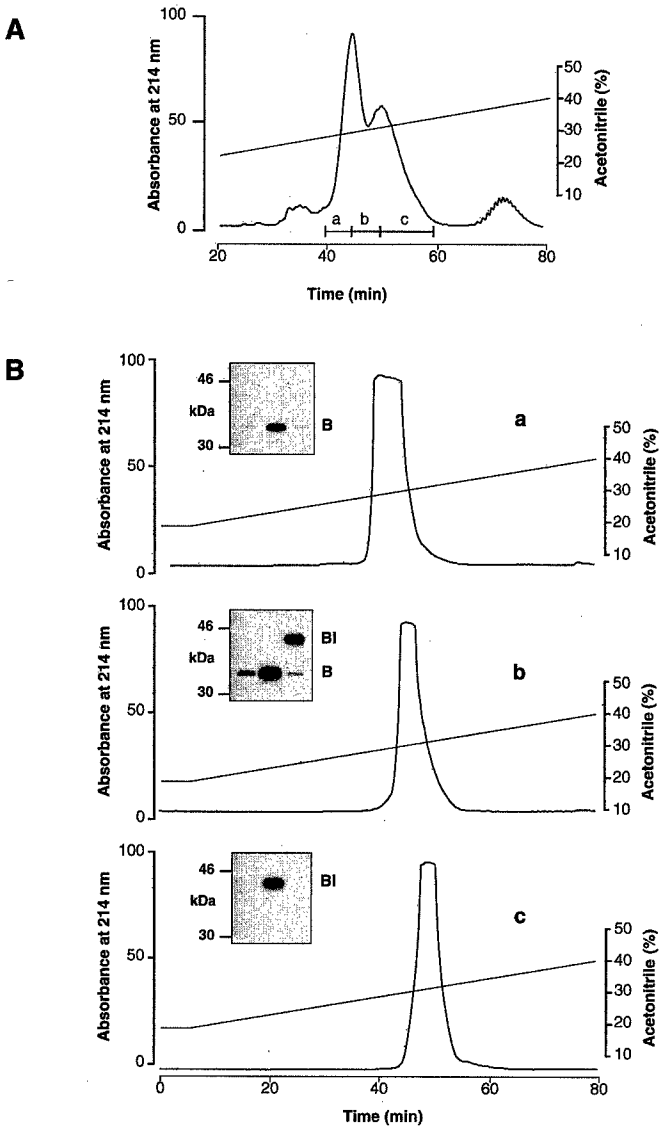

FIG. 8. **Purification of IGF-1·IGFBP-2 complexes.** *A*, following reduction and alkylation, the abG^{1}IGF-1/IGFBP-2 photolysis reaction mixture was purified on a C_{18} column equilibrated in 0.1% trifluoroacetic acid and 24% acetonitrile. *B*, the major components (*a–c*) of the elution profile obtained in *A* were re-chromatographed separately using a shallow acetonitrile gradient. *Insets*, fractions from each run were analyzed by immunoblotting with anti-IGFBP-2 antibody. *B*, IGFBP-2; *BI*, IGF-1·IGFBP-2 complex.

not shown). Two major peaks were observed in the low pH elution of the column. The first peak exhibited a mass of 2595.7 Da when analyzed by MALDI-TOF-MS (Fig. 10*B*). When corrected for the mass of the biotin and remaining cross-linker residues from the bed moiety (653.3 Da), this corresponded to a BP2T fragment of 1942.3 Da (Fig. 10*B*). This coincides with tryptic peptide 212–227 (predicted mass of 1942.2 Da) from the C terminus of IGFBP-2. MALDI-TOF-MS analysis of the second peak eluted from the avidin column revealed the presence of a major signal at 1667.4 Da. When corrected for cross-linker/biotin, the BP2T fragment had a mass of 1014.1 Da, which did not correspond to any tryptic peptides present in rhIGFBP-2 (Fig. 10*B*). However, this mass did correspond to the first 9 residues of the BP2T fragment already identified (residues 212–220). These findings suggest that photoaffinity labeling with the bed reagent resulted in partial peptide bond cleavage at the site of covalent insertion. The potential for peptide bond cleavage during photoaffinity labeling has previously been suggested in the literature (37). This conclusion is further supported by the data presented in Fig. 7*B* (*lanes 4–6*), where we detected an IGFBP-2 fragment that was reactive with NeutrAvidin™-peroxidase. Taken together, these results suggest that the site of insertion may be residue 220 of IGFBP-2 (Fig. 11*A*).

DISCUSSION

In this report, we present evidence for a C-terminal contact site on IGFBP-2 for IGF-1 based on direct photoaffinity labeling studies with two unique N-terminally modified photoaffinity derivatives of IGF-1. We interpret these findings as an indication of the presence of a high affinity binding site for IGF-1 within the C terminus of IGFBP-2. Consistent with this finding are a number of reports describing the C terminus of IGFBP-2 as the domain containing the high affinity IGF-binding site. Wang *et al.* (38) and Ho and Baxter (39) each identified C-terminal fragments of IGFBP-2 with high affinity IGF-binding activity. In preliminary studies, we have characterized a 15.8-kDa C-terminal fragment of rhIGFBP-2 from our transfected Chinese hamster ovary cell cultures that exhibits an affinity for IGF-1 identical to that of intact rhIGFBP-2.[2] This fragment lacks N-terminal and mid-region epitopes based on tryptic peptide mapping studies. Additional support for the C terminus as the site of IGF binding stems from studies of Brinkman *et al.* (40), who deleted the last 20 amino acids from the C terminus of IGFBP-1 and thereby abolished IGF-1-binding activity. Similarly, Forbes *et al.* (41) generated a series of four sequential C-terminal truncation mutants of bovine IGFBP-2 and concluded that residues 222–236 are required for high affinity IGF interactions. Finally, Schuller *et al.* (42) prepared monoclonal antibodies to residues 188–196 and 222–227 of IGFBP-1 that blocked IGF-1 binding. These investigators concluded that the regions surrounding these epitopes were important for IGF binding.

Introduction of photoactivable aryl azide moieties within the IGFBP-binding domain on IGF-1 (residues 1–3 and 49–51) resulted in the selective photoaffinity labeling of two separate sites in the C terminus of IGFBP-2, within tryptic peptides 266–287 (abG^{1}IGF-1) and 212–227 (bedG^{1}IGF-1) (Fig. 11*A*). The labeling of these different sites can be attributed to the different side chain lengths of the two IGF-1 photoprobes. abG^{1}IGF-1 contains an azidobenzoyl moiety and thus lacks an appreciable side chain between the α-amino group of Gly^1 and the aryl azide. In this case, the aryl azide resides near the outer edge of the IGF-1-binding domain, defining the site of contact for Gly^1. The longer, more flexible side chain present on the aryl azide in bedG^{1}IGF-1 has the potential to define a contact site within the vicinity of the other residues of the IGFBP-binding domain, including Glu^3, which plays an essential role in maintaining high affinity binding to the IGFBPs (43). Although we cannot rule out the possibility that this side chain results in the labeling of regions of the IGFBPs outside the IGF-binding domain, we believe that the likelihood of this occurring is minimal based on the previous identifications of C-terminal binding activity described above. Given the globular nature of the IGFBPs and the disulfide bonding pattern in this domain (Fig. 11*B*) (41), these two sites are likely to be closely apposed in three-dimensional space. Although the two photoprobes labeled sites within the C terminus of IGFBP-2 that are separated by ~40 amino acids in the primary sequence, these sites are likely to be much closer when the secondary structure of the protein is taken into consideration (Fig. 11*B*). Indeed, the two labeled sites cannot be farther apart than the total length of the two photoprobe spacer arms combined (~300 nm).

Based on chemical modifications, site-directed mutagenesis

[2] M. J. Horney and S. A. Rosenzweig, manuscript in preparation.

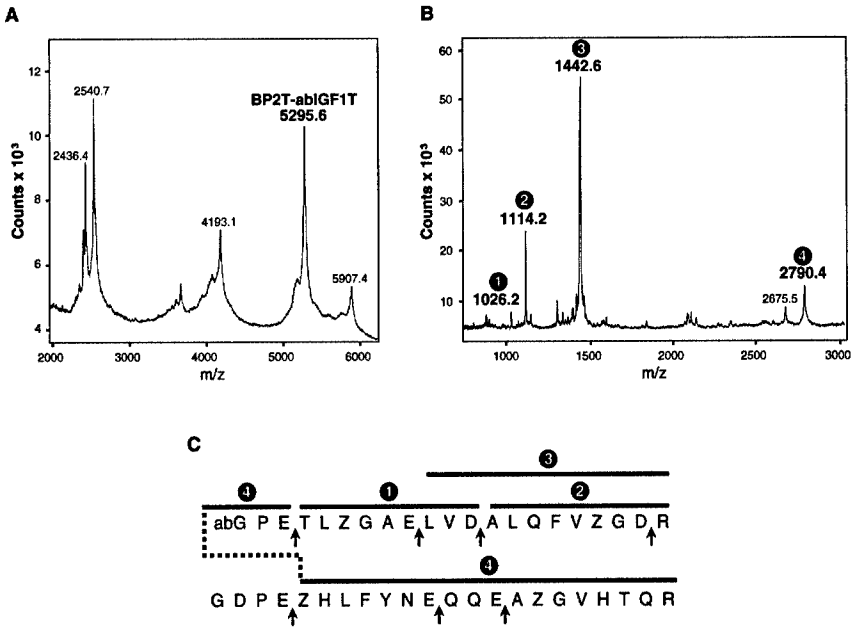

FIG. 9. **Analysis of abG¹IGF-1·IGFBP-2 photoaffinity-labeled complex.** *A*, shown is a MALDI-TOF mass spectrum of a unique peak having a mass (5295.6 Da) that lacks correspondence to IGF-1 or IGFBP-2 tryptic peptides. *B*, the column fraction containing the 5295.6-Da fragment was dried and subdigested with *S. aureus* V8 protease. Shown is the MALDI-TOF mass spectrum of the digestion products. *C*, the peptides identified in the V8 digest in *B* are indicated.

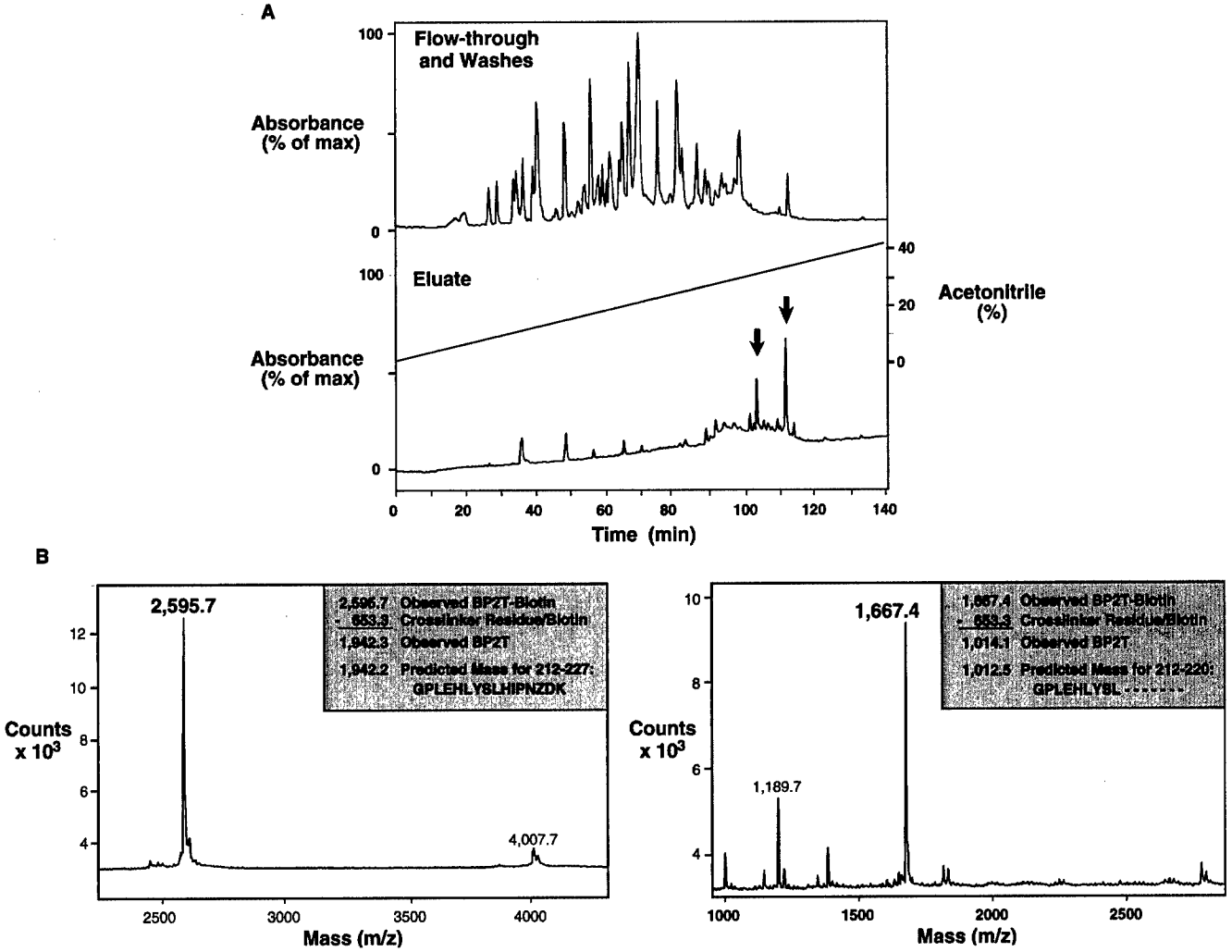

FIG. 10. **Analysis of bedG¹IGF-1·IGFBP-2 photoaffinity-labeled complex.** *A*, elution profile of the reduced, alkylated, and trypsin-digested photolysis reaction mixture following chromatography on a column of monomeric avidin. Shown are the HPLC column profiles of the column flow-through/washes and eluate. *B*, MALDI-TOF mass spectrum of the peaks identified by *arrows* in *A*. The first peak exhibited a mass of 2595.7 Da. After correcting the observed mass for the associated biotin and spacer, it was identified as tryptic peptide 212–227. The second biotinylated component (*second arrow*) was identified as having a mass of 1014.1 Da, which corresponds to a truncated form of the same tryptic peptide (residues 212–220) and suggests rupture of the peptide backbone of IGFBP-2 during photoincorporation. This finding explains the composition of the smaller band observed in Fig. 7*B* (loss of ~7 kDa; residues 221–289). *Z*, pyridylethylated cysteine.

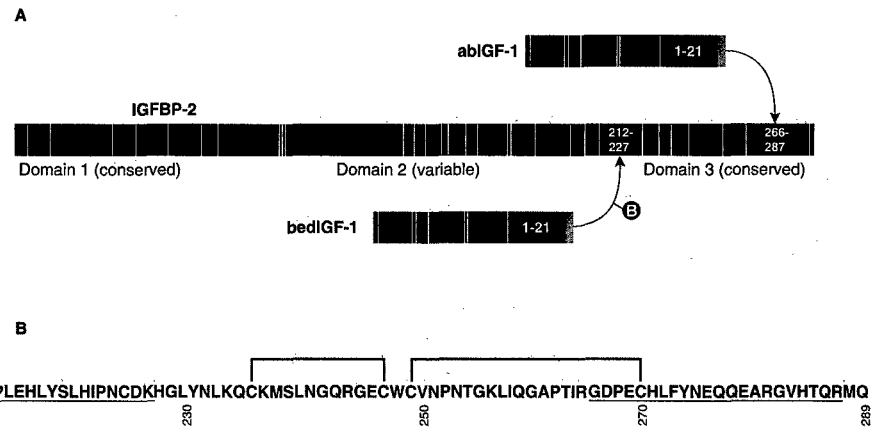

FIG. 11. **Sites of photoincorporation into IGFBP-2.** *A*, depiction of sites of photoincorporation of abG[1]IGF-1 and bedG[1]IGF-1 into IGFBP-2. *White lines* represent sites of trypsin cleavage. *B*, detailed view of the C-terminal region (residues 210–289) showing the known disulfide bonding pattern (41). *Underlined* peptides represent tryptic peptides identified as sites of photoincorporation.

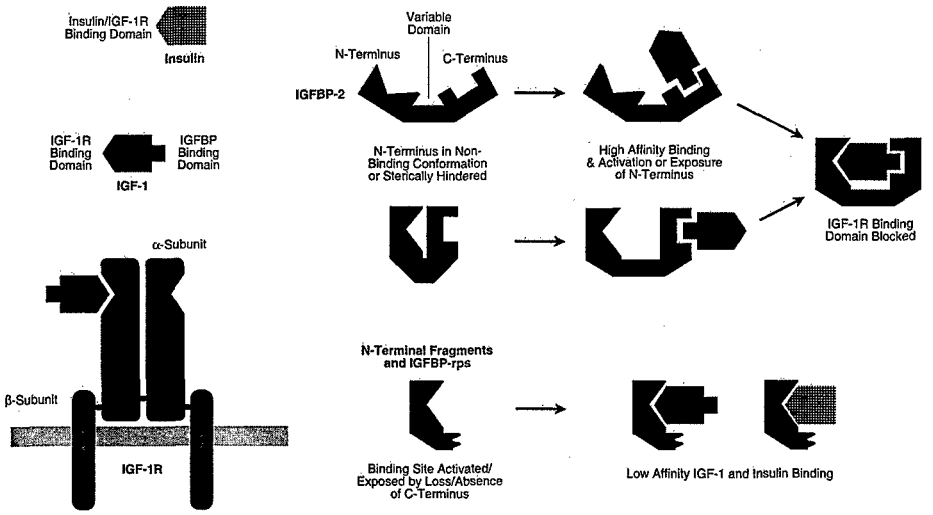

FIG. 12. **Model of IGF-1/IGF-1R binding inhibition by IGFBP-2.** Based on the data presented, the IGFBP-binding domain on IGF-1 interacts with the C terminus of IGFBP-2. Once this complex is formed, the IGF-1R-binding domain on IGF-1 then binds to the N terminus of IGFBP-2. *IGFBP-rps*, IGFBP-related proteins.

studies, and the identification of fragments with IGF-binding activity, the N terminus of the IGFBPs has also been described as the site of the IGF-binding domain. Iodination studies on bovine IGFBP-2 in isolation or as a complex bound to IGF-2 resulted in efficient iodination of Tyr residues at positions 71, 98, 213, 226, and 269; Tyr^{60} was protected from iodination by bound IGF-2 (44). Huhtala *et al.* (45) isolated a 21-kDa N-terminal fragment of IGFBP-1 that retained some IGF-1-binding activity. More recently, Kalus *et al.* (46) reported that N-terminal fragments of IGFBP-5 representing residues 1–104 and 40–92 exhibit weak IGF-binding activity. Based on NMR studies, they defined a hydrophobic patch comprising residues 49, 50, 62, and 68–75 that potentially represents the primary IGF-binding site on IGFBP-5. This hypothesis was subsequently tested by the construction of full-length IGFBP-5 and IGFBP-3 mutants in which combined substitutions at residues 68, 69, 70, 73, and 74 resulted in a >1000-fold reduction in binding affinity (47). Contrary to these mutagenesis results, Ständker *et al.* (48) reported that the C terminus of IGFBP-5 contains the IGF-binding domain based on the isolation of a naturally occurring, biologically active truncation of IGFBP-5. The observation by Yamanaka *et al.* (24) that insulin can bind to (and be chemically cross-linked into) the N terminus of IGFBP-related protein-1 may provide further insight into the mechanism of IGF/IGFBP interactions, suggesting the notion that the N- and C-terminal domains may both interact with IGF-1, but with differing specificity and function (49).

In the context of the present findings, we propose the following model (Fig. 12) based on the idea that two binding sites for IGF-1 exist on the IGFBPs. The first is a high affinity, high specificity site (C terminus) responsible for binding selectivity for IGF-1 via its IGFBP-binding domain. The second low affinity site (N terminus) binds to IGF-1 via its IGF-1R-binding domain and thus plays a role in blocking IGF-1 binding to the IGF-1R. This model would likely require a conformational change to take place within the N terminus following IGF binding to the C terminus. Evidence to support this comes from NMR analyses of IGF·IGFBP complexes (50, 51). It is possible to speculate that such conformational changes may reflect the ability of the IGFBP, following initial binding to the N terminus (IGFBP-binding domain) of IGF-1, to interact with the IGF-1R domain of IGF-1. This could provide a steric mechanism through which inhibition of IGF-1R activation is accomplished. This in turn explains low affinity insulin binding to the N terminus of IGFBP-related protein-1 (9). In addition, a conformational change explains why des-1–3-IGF-1 does not bind the IGFBPs well, even though it still contains an intact IGF-1R-binding domain.

This scheme may serve to explain how N-terminal fragments and truncation mutants of the IGFBPs are able to bind to IGF-1. This would also support a steric hindrance-based model of IGFBP inhibition of IGF-1 action at the IGF-1R. Following high affinity binding between the IGFBP-binding domain on IGF-1 and its contact site within the C terminus of IGFBP-2, the ensuing conformational rearrangement enables high affinity interaction of the N terminus of IGFBP-2 with the IGF-1R binding domain on IGF-1. Obviously, this is one of several potential models one might propose; confirmation of any such model will require a more definitive understanding of the three-dimensional structure of the IGFBPs. Future photolabel-

ing studies with abK[27]IGF-1 and bedK[27]IGF-1 may aid in addressing the issue of whether there are N-terminal contact sites on the IGFBPs for the IGF-1R-binding domain on IGF-1.

Based on their ability to block IGF actions, we have chosen to pursue the design of IGF antagonists based on the structure of the IGF-binding domain on the IGFBPs. This clearly requires more detailed information than is currently available concerning IGFBP structure. We have employed a photoaffinity labeling approach as a means of identifying the IGF-1 site of contact on IGFBP-2. To this end, a photoreactive derivative of IGF-1 was prepared, exploiting the reactivity of primary amines in the protein to covalently attach an aryl azide moiety within the IGFBP-binding domain. This approach has been used for many photoaffinity labeling studies, including the insulin (52) and IGF-1 (36) receptors. It has the drawback of incorporating a bulky group into the ligand, which may alter its binding characteristics. However, in the case of abG[1]IGF-1 and bedG[1]IGF-1, we did not observe a significant alteration in binding affinity for IGFBP-2. An alternative approach would be to utilize an intrinsically labeled IGF-1 derivative containing a photoactivable moiety at an aromatic amino acid. This has been reported for the identification of an insulin contact point on the insulin receptor (22). To accomplish this, Phe[B25] in the receptor-binding domain of insulin was replaced with *p*-azidophenylalanine to generate (B25-*p*-azidophenylalanine-α-carboxamide)-insulin. To apply a similar strategy to studies with IGF-1 would require considerable peptide semi-syntheses. Instead, we chose the alternative of incorporating an extrinsic photoactivable moiety into the α-amino group of Gly[1], a residue that constitutes part of the IGFBP-binding domain on IGF-1. Of the two photoprobes employed, the use of SBED to biotinylate the site of IGF-1 photoincorporation provided a more direct approach to the identification of the photocross-linked tryptic peptide. This represents the first report of the successful use of this reagent in photolabeling a ligand-binding site.

In conclusion, this study represents the first report defining a contact site between IGF-1 and IGFBP-2. We propose to exploit this structural information to develop unique antagonists of the IGFs as important therapeutic adjuncts in the prevention/treatment of various cancers and the complications of diabetes. Small peptides comprising the proposed IGF-binding site would serve as stable, protease-resistant analogs of the IGFBPs (IGFBP mimetics). These compounds will be designed to block IGF action and will serve as important templates for the future design of peptidomimetics. To this end, IGF-1 antagonists should provide important therapeutic adjuncts in the prevention/treatment of these diseases.

Acknowledgments—We thank Genentech, Inc. for generously providing recombinant human IGF-1; Dr. Jörg Landwehr for human IGFBP-2 cDNA; and Dr. David T. Kurtz (Medical University of South Carolina) for pMT2 cDNA, DG44 cells, and advice on the generation of human IGFBP-2-expressing Chinese hamster ovary cells. We especially thank Helga Hsu and Dr. Cecil C. Yip (University of Toronto) for many productive discussions. We also thank Dr. Kevin Schey (Medical University of South Carolina) for critical comments on the interpretation of MALDI-TOF-MS and electrospray ionization mass spectrometric data, Dr. Erika Büllesbach (Medical University of South Carolina) for helpful comments concerning synthesis conditions, and Dr. John Oatis (Medical University of South Carolina) for reduction and alkylation protocols. Finally, we thank the other members of the Rosenzweig laboratory for many helpful comments.

REFERENCES

1. Daughaday, W. H., and Rotwein, P. (1989) *Endocr. Rev.* **10,** 68–91
2. Baserga, R. (1995) *Cancer Res.* **55,** 249–252
3. Louvi, A., Accili, D., and Efstratiadis, A. (1997) *Dev. Biol.* **189,** 33–48
4. Ludwig, T., Le Borgne, R., and Hoflack, B. (1995) *Trends Cell Biol.* **5,** 202–205
5. Holly, J. M. P. (1993) in *Growth Hormone and Insulin-like Growth Factor I in Human and Experimental Diabetes* (Flyvjberg, A., Orskov, H., and Alberti, G., eds) pp. 47–76, John Wiley & Sons Ltd., Chichester, United Kingdom
6. Clemmons, D. R., Jones, J. I., Busby, W. H., and Wright, G. (1993) *Ann. N. Y. Acad. Sci. U. S. A.* **692,** 10–21
7. Jones, J. I., and Clemmons, D. R. (1995) *Endocr. Rev.* **16,** 13–34
8. Long, L., Rubin, R., Baserga, R., and Brodt, P. (1995) *Cancer Res.* **55,** 1006–1009
9. Chan, J. M., Stampfer, M. J., Giovannucci, E., Gann, P. H., Ma, J., Wilkinson, P., Hennekens, C. H., and Pollak, M. (1998) *Science* **279,** 563–566
10. Hankinson, S. E., Willett, W. C., Colditz, G. A., Hunter, D. J., Michaud, D. S., Deroo, B., Rosner, B., Spitzer, F. E., and Pollak, M. (1998) *Lancet* **351,** 1393–1396
11. Buckbinder, L., Talbott, R., Velasco-Miguel, S., Takenaka, I., Faha, B., Seizinger, B. R., and Kley, N. (1995) *Nature* **377,** 646–649
12. Burns, T. F., and El-Deiry, W. S. (1999) *J. Cell. Physiol.* **181,** 231–239
13. Horney, M. J., Shirley, D. W., Kurtz, D. T., and Rosenzweig, S. A. (1998) *Am. J. Physiol.* **274,** F1045–F1053
14. Humbel, R. E. (1990) *Eur. J. Biochem.* **190,** 445–462
15. Blundell, T. L., Bedarkar, S., Rinderknecht, E., and Humbel, R. E. (1978) *Proc. Natl. Acad. Sci. U. S. A.* **75,** 180–184
16. Cooke, R. M., Harvey, T. S., and Campbell, I. D. (1991) *Biochemistry* **30,** 5484–5491
17. Szabo, L., Mottershead, D. G., Ballard, F. J., and Wallace, J. C. (1988) *Biochem. Biophys. Res. Commun.* **151,** 207–214
18. Cascieri, M. A., Chicchi, G. G., Applebaum, J., Green, B. G., Hayes, N. S., and Bayne, M. L. (1989) *J. Biol. Chem.* **264,** 2199–2202
19. Clemmons, D. R., Dehoff, M. L., Busby, W. H., Bayne, M. L., and Cascieri, M. A. (1992) *Endocrinology* **131,** 890–895
20. Kiefer, M. C., Ioh, R. S., Bauer, D. M., and Zapf, J. (1991) *Biochem. Biophys. Res. Commun.* **176,** 219–225
21. Kiefer, M. C., Masiarz, F. R., Bauer, D. M., and Zapf, J. (1991) *J. Biol. Chem.* **266,** 9043–9049
22. Kurose, T., Pashmforoush, M., Yoshimasa, Y., Carroll, R., Schwartz, G. P., Burke, G. T., Katsoyannis, P. G., and Steiner, D. F. (1994) *J. Biol. Chem.* **269,** 29190–29197
23. Hwa, V., Oh, Y., and Rosenfeld, R. G. (1999) *Endocr. Rev.* **20,** 761–787
24. Yamanaka, Y., Wilson, E. M., Rosenfeld, R. G., and Oh, Y. (1997) *J. Biol. Chem.* **272,** 30729–30734
25. Baxter, R. C. (2000) *Am. J. Physiol.* **278,** E967–E976
26. Galardy, R. E., Craig, L. C., Jamieson, J. D., and Printz, M. P. (1974) *J. Biol. Chem.* **249,** 3510–3518
27. Binkert, C., Landwehr, J., Mary, J.-L., Schwander, J., and Heinrich, G. (1989) *EMBO J.* **8,** 2497–2502
28. Forsberg, G., Gunnar, P., Ekebacke, A., Josephson, S., and Hartmanis, M. (1990) *Biochem. J.* **271,** 357–363
29. Urlaub, G., Kas, E., Carothers, A. M., and Chasin, L. A. (1983) *Cell* **33,** 405–412
30. Kaufman, R. J., Davies, M. V., Pathak, V. K., and Hershey, J. W. (1989) *Mol. Cell. Biol.* **9,** 946–958
31. Bourner, M. J., Busby, W. H., Jr., Siegel, N. R., Krivi, G. G., McCusker, R. H., and Clemmons, D. R. (1992) *J. Cell. Biochem.* **48,** 215–226
32. Han, J. C., and Han, G. Y. (1994) *Anal. Biochem.* **220,** 5–10
33. Liu, C., and Bowers, L. D. (1997) *J. Mass Spectrom.* **32,** 33–42
34. Honegger, A., and Humbel, R. E. (1986) *J. Biol. Chem.* **261,** 569–575
35. Laemmli, U. K. (1970) *Nature* **227,** 680–685
36. Yip, C. C., Hsu, H., Olefsky, J., and Seely, L. (1993) *Peptides (Elmsford)* **14,** 325–330
37. Bayley, H., and Staros, J. V. (1984) in *Azides and Nitrenes: Reactivity and Utility* (Scriven, E. F. V., ed) pp. 434–490, Academic Press, Inc., Orlando, FL
38. Wang, J. F., Hampton, B., Mehlman, T., Burgess, W. H., and Rechler, M. M. (1988) *Biochem. Biophys. Res. Commun.* **157,** 718–726
39. Ho, P. J., and Baxter, R. C. (1997) *Endocrinology* **138,** 3811–3818
40. Brinkman, A., Kortleve, D. J., Zwarthoff, E. C., and Drop, S. L. (1991) *Mol. Endocrinol.* **5,** 987–994
41. Forbes, B. E., Turner, D., Hodge, S. J., McNeil, K. A., Forsberg, G., and Wallace, J. S. (1998) *J. Biol. Chem.* **273,** 4647–4652
42. Schuller, A. G., Lindenbergh-Kortleve, D. J., de Boer, W. I., Zwarthoff, E. C., and Drop, S. L. (1993) *Growth Regulation* **3,** 32–34
43. Laajoki, L. G., Francis, G. L., Wallace, J. C., Carver, J. A., and Keniry, M. A. (2000) *J. Biol. Chem.* **275,** 10009–10015
44. Hobba, G. D., Forbes, B. E., Parkinson, E. J., Francis, G. L., and Wallace, J. C. (1996) *J. Biol. Chem.* **271,** 30529–30536
45. Huhtala, M.-L., Koistinen, R., Palomäki, P., Partanen, P., Bohn, H., and Seppälä, M. (1986) *Biochem. Biophys. Res. Commun.* **141,** 263–270
46. Kalus, W., Zweckstetter, M., Renner, C., Sanchez, Y., Georgescu, J., Grol, M., Demuth, D., Schumacher, R., Dony, C., Lang, K., and Holak, T. A. (1998) *EMBO J.* **17,** 6558–6572
47. Imai, Y., Moralez, A., Andag, U., Clarke, J. B., Busby, W. H., Jr., and Clemmons, D. R. (2000) *J. Biol. Chem.* **275,** 18188–18194
48. Ständker, L., Wobst, P., Mark, S., and Forssmann, W.-G. (1998) *FEBS Lett.* **441,** 281–286
49. Spencer, E. M., and Chan, K. (1995) *Prog. Growth Factor Res.* **6,** 209–214
50. Jansson, M., Hallén, D., Koho, H., Andersson, G., Berghard, L., Heidrich, J., Nyberg, E., Uhlén, M., Kördel, J., and Nilsson, B. (1997) *J. Biol. Chem.* **272,** 8189–8197
51. Jansson, M., Andersson, G., Uhlén, M., Nilsson, B., and Kördel, J. (1998) *J. Biol. Chem.* **273,** 24701–24707
52. Yip, C. C., Yeung, W. T., and Moule, M. L. (1980) *Biochemistry* **19,** 70–76